Synthesis, Experimental and ab Initio Theoretical Vibrational Circular Dichroism, and Absolute Configurations of Substituted Oxiranes

Simeon T. Pickard,[†] Howard E. Smith,*[,†] Prasad L. Polavarapu,*[,†] Thomas M. Black,[†] Arvi Rauk,*[,‡] and Danya Yang[‡]

Contribution from the Departments of Chemistry, Vanderbilt University, Nashville, Tennessee 37235, and University of Calgary, Calgary, Alberta T2N 1N4, Canada.
Received February 3, 1992

Abstract: Both enantiomers of *trans*-2,3-dimethyloxirane-d_0, *trans*-2,3-dimethyloxirane-2-d_1, and *trans*-2,3-dimethyloxirane-2,3-d_2 are synthesized. Vibrational circular dichroism (VCD) spectra for these compounds are obtained in the 1600–700-cm^{-1} region. Ab initio theoretical calculations using the localized molecular orbital method (LMO–VCD) and the vibronic coupling theoretical method (VCT) are also obtained for these molecules. A comparison of the theoretical VCD predictions with the corresponding experimental observations demonstrates that the observed VCD features are satisfactorily reproduced by the theories, indicating that absolute configurations can be confidently determined using vibrational circular dichroism.

Introduction

trans-2,3-Dimethyloxirane has attracted much attention for electronic and vibrational optical activity studies[1] due to its conformational rigidity, small size, and potential for serving as a bench mark for rigorous theoretical investigations.[2] The enantiomers of its 2-d_1 and 2,3-d_2 isotopomers were not synthesized before but are valuable for VCD studies in establishing the vibrational origin of observed bands and in separating the modes which otherwise have a strong mixing.

In order to use vibrational circular dichroism (VCD) for determining the absolute configuration, the observed VCD bands have to be interpreted using suitable and reliable theoretical models. Quantum theoretical methods are absolutely necessary for reliable predictions, although they demand considerable computer time. Four such methods are currently available: the magnetic field perturbation (MFP) theory,[3-5] the vibronic coupling theory (VCT),[6] the localized molecular orbital (LMO) theory,[7-9] and the localized orbital–local origin (LORG) theory.[10] Although each of them has some characteristic practical limitations, the reliability of these methods in predicting qualitatively correct spectra is expected to be very good. To establish this reliability, the theoretical model predictions have to be critically compared to the experimental data and a large data base of such comparisons is required. This goal can be met only for small optically active molecules for which ab initio calculations can be performed. Besides 2,3-dimethyloxirane, there are only a limited number of molecules for which this has been accomplished: 2,3-dideuteriooxirane,[11-13] 1,2-dideuteriocyclopropane,[14,15] methyloxirane,[2,16] methylthiirane,[17-20] 2,3-dimethylthiirane,[20] 2,3-dimethylthiirane-2,3-d_2,[20] and ethanol-α-d.[21] From this viewpoint, the synthesis and VCD data of the deuterated oxiranes presented here are important. The VCD spectra of *trans*-2,3-dimethyloxirane-d_0 were reported before,[1] but those of the 2-d_1 and 2,3-d_2 isotopomers were not available.

In this paper we present a novel synthetic scheme for preparing both enantiomers of *trans*-2,3-dimethyloxirane-d_0, *trans*-2,3-dimethyloxirane-2-d_1, and *trans*-2,3-dimethyloxirane-2,3-d_2. We apply the LMO and VCT models to predict the VCD spectra. The experimental and ab initio theoretical VCD spectra are presented and critically compared.

Results and Discussion

As shown in Scheme I, preparation of the enantioenriched (2*S*,3*S*)-*trans*-dimethyloxirane[22] [(2*S*,3*S*)-**5a**] (Table I) proceeds from crotyl alcohol,[23] *trans*-2-buten-1-ol (**2a**), by way of the Sharpless epoxidation reaction.[24] A similar reaction sequence was used to prepare enantioenriched deuterium-substituted trans oxiranes in which the deuterium atoms are on the ring carbon atoms. Thus, the corresponding deuterium-substituted alcohols,

Scheme I

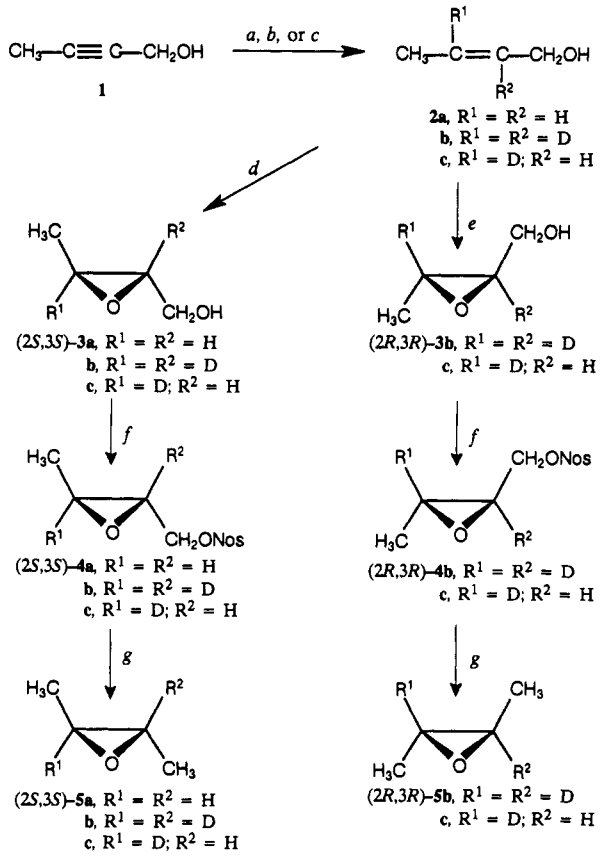

[a-g] Reagent (yield): *a*, lithium aluminum hydride in THF and then water (55%); *b*, lithium aluminum deuteride in THF and then deuterium oxide (65%); *c*, lithium aluminum hydride in THF and then deuterium oxide (61%); *d*, diethyl L-(+)-tartrate, titanium isopropoxide, *tert*-butylhydroperoxide in methylene chloride–isooctane (43–55%, chemical purity 90–95%); *e*, diethyl D-(−)-tartrate, titanium isopropoxide, *tert*-butylhydroperoxide in methylene chloride-isooctane (43–47%, chemical purity 85–95%); *f*, *p*-nitrobenzenesulfonyl chloride in methylene chloride with diisopropylamine (50–68%); *g*, sodium cyanoborohydride in hexamethylphosphoramide, HMPA (14–40%).

[†] Vanderbilt University.
[‡] University of Calgary.

(1) Black, T. M.; Bose, P. K.; Polavarapu, P. L.; Barron, L. D.; Hecht, L. *J. Am. Chem. Soc.* **1990**, *112*, 1479–1480.

0002-7863/92/1514-6850$03.00/0

Table I. Enantioenriched *trans*-2,3-Dimethyloxiranes[a]

	$[\alpha]^{23-25}_D$, deg (neat, 0.5 dm)	% ee
(2*S*,3*S*)-2,3-dimethyloxirane [(2*S*,3*S*)-**5a**]	−19.6	83[b]
(2*S*,3*S*)-2,3-dimethyloxirane-2,3-d_2 [(2*S*,3*S*)-**5b**]	−19.5	80[c]
(2*R*,3*R*)-2,3-dimethyloxirane-2,3-d_2 [(2*R*,3*R*)-**5b**]	+18.1	75[d]
(2*S*,3*S*)-2,3-dimethyloxirane-2-*d* [(2*S*,3*S*)-**5c**]	−19.2	85[d]
(2*R*,3*R*)-2,3-dimethyloxirane-2-*d* [(2*R*,3*R*)-**5c**]	+19.0	85[c]

[a] Bp 54–56 °C. [b] Previously reported as $[\alpha]^{25}_D$ −47.02° (neat, 1 dm), 100% ee. [c] Based on the % ee of its enantiomer; rounded to the nearest 5% and accurate to ±5%. [d] Determined on the basis of its 300-MHz ^{1}H NMR spectrum in the presence of a chiral lanthanide shift reagent (cf. ref 33) in benzene-d_6; rounded to the nearest 5% and accurate to ±5%.

Scheme II

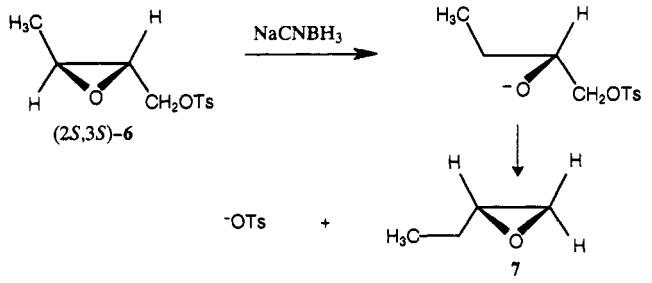

trans-2-buten-1-ol-*2,3-d*$_2$ (**2b**) and *trans*-2-buten-1-ol-*3-d* (**2c**), were prepared by lithium aluminum deuteride or hydride reduction of 2-butyn-1-ol (**1**). In a polar solvent such as tetrahydrofuran (THF), the reduction is known to be stereoselective,[25] and

Scheme III

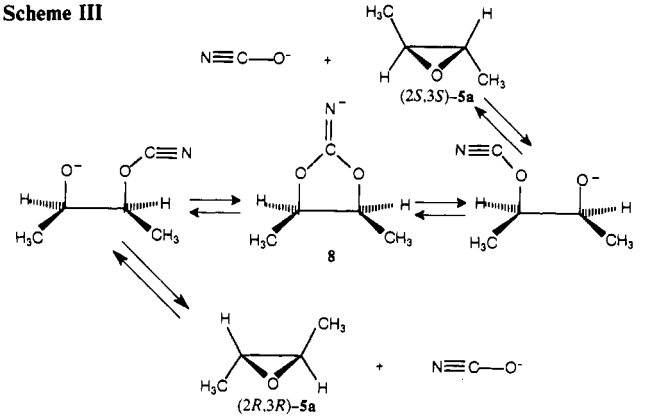

trans-2-buten-1-ol-*2,3-d*$_2$ (**2b**) and *trans*-2-buten-1-ol-*3-d* (**2c**) were formed respectively by reduction with lithium aluminum deuteride and then quenching with deuterium oxide or reduction with lithium aluminum hydride and then quenching with deuterium oxide. In the first stage of the reaction, the initial transfer of deuteride or hydride ion from the reducing agent was predominantly to the carbon atom β to the alcohol group,[26] but in the preparation of **2c**, a substantial amount of *trans*-2-buten-1-ol-*2-d*, the regioisomer of **2c**, was also formed. The symmetry of the *trans*-2,3-dimethyloxiranes ultimately formed from **2c** made this contamination of the alcohol of no consequence.

After epoxidation of the crotyl alcohols using the Sharpless asymmetric synthesis with diethyl L-(+)- or D-(−)-tartrate as the chiral auxiliary,[24] removal of the hydroxyl group was achieved by way of reduction of the corresponding sulfonate ester using sodium cyanoborohydride.[27] Initially, an attempt was made to utilize the *p*-toluenesulfonate (tosylate) esters of the chiral alcohols. With the tosylate of (2*S*,3*S*)-3-(hydroxymethyl)-2-methyloxirane [(2*S*,3*S*)-**6**] as the model system, the major product, (2*S*,3*S*)-*trans*-2,3-dimethyloxirane [(2*S*,3*S*)-**5a**], contained about 5% of an impurity which was not easily removed and which from its ^{1}H NMR spectrum appeared to be 2-ethyloxirane (**7**). This constitutional isomer of **5a** may arise, as shown in Scheme II, from attack of the hydride-transfer reagent at the epoxide carbon atom remote from the tosyl group followed by displacement of the tosyl group by the oxygen anion.

When the more reactive *p*-nitrobenzenesulfonate (nosylate) esters were used as substrates for removal of the hydroxyl group by reduction, no product corresponding to **7** was detected in the ^{1}H NMR spectra of the crude reaction product. The Sharpless oxidation reaction, however, did not proceed with complete stereoselectivity. Recrystallization of the nosylate derivatives caused enrichment of the racemic form in the recovered crystals, and thus large volumes of recrystallization solvents were avoided.

For reduction of the nosylate esters, sodium cyanoborohydride was the source of hydride ion and hexamethylphosphoramide[27] (HMPA) was the solvent used. When a diethylene glycol–HMPA mixture was used as reaction solvent, the yield of the reaction was significantly improved. This improvement seemed to result from the improved solubility of the sodium cyanoborohydride and the sulfate salt produced in the reaction. The improved yield, however, was accompanied by substantial racemization, sometimes as high as 50%. It is speculated that water, which is very difficult to remove completely from the diethylene glycol, caused the formation of a small amount of cyanate anion, which catalyzed the racemization of the epoxides by a mechanism (Scheme III) in which the symmetrical intermediate **8** was formed. This reaction is analogous to that for the formation of thiiranes by reaction of sodium thiocyanate with the corresponding oxirane.[28] In order

(2) Rauk, A.; Yang, D. *J. Phys. Chem.* **1992**, *96*, 437–446.
(3) (a) Galwas, P. A. Ph.D. Thesis, Cambridge University, Cambridge, U.K., 1983. (b) Buckingham, A. D.; Fowler, P. W.; Galwas, P. A. *Chem. Phys.* **1987**, *112*, 1–14.
(4) (a) Stephens, P. J. *J. Phys. Chem.* **1985**, *89*, 748–752. (b) Stephens, P. J. *J. Phys. Chem.* **1987**, *91*, 1712–1715.
(5) Stephens, P. J.; Jalkanen, K. J.; Amos, R. D.; Lazzeretti, P.; Zanasi, R. *J. Phys. Chem.* **1990**, *94*, 1811.
(6) Nafie, L. A.; Freedman, T. B. *J. Chem. Phys.* **1983**, *78*, 7108.
(7) Walnut, T. W.; Nafie, L. A. *J. Chem. Phys.* **1977**, *67*, 1501–1510.
(8) Nafie, L. A.; Walnut, T. W. *Chem. Phys. Lett.* **1977**, *49*, 441–446.
(9) Nafie, L. A.; Polavarapu, P. L. *J. Chem. Phys.* **1981**, *75*, 2935–2944.
(10) Hansen, A. E.; Stephens, P. J.; Bouman, T. D. *J. Phys. Chem.* **1991**, *95*, 4255–4262.
(11) (a) Dutler, R. Ph.D. Dissertation, University of Calgary, Calgary, Alberta, Canada, 1988. (b) Dutler, R.; Rauk, A. *J. Am. Chem. Soc.* **1989**, *111*, 6957–6966.
(12) Stephens, P. J.; Jalkanen, K. J.; Kawiecki, R. W. *J. Am. Chem. Soc.* **1990**, *112*, 6518–6529.
(13) Polavarapu, P. L.; Bose, P. K. *J. Chem. Phys.* **1990**, *93*, 7524–7525.
(14) Jalkanen, K. J.; Kawiecki, R. W.; Stephens, P. J.; Amos, R. D. *J. Phys. Chem.* **1990**, *94*, 7040–7055.
(15) Polavarapu, P. L.; Bose, P. K. *J. Phys. Chem.* **1991**, *95*, 1606–1608.
(16) Kawiecki, R. W.; Devlin, F.; Stephens, P. J.; Amos, R. D.; Handy, N. C. *Chem. Phys. Lett.* **1988**, *145*, 411–417.
(17) Dothe, H.; Lowe, M. A.; Alper, J. S. *J. Phys. Chem.* **1988**, *92*, 6246–6249.
(18) Amos, R. D.; Handy, N. C.; Palmieri, P. *J. Chem. Phys.* **1990**, *93*, 5796–5804.
(19) (a) Polavarapu, P. L.; Bose, P. K.; Pickard, S. T. *J. Am. Chem. Soc.* **1991**, *113*, 43–48. (b) Polavarapu, P. L.; Hess, B. A.; Schaad, L. J.; Henderson, D. O.; Fontana, L. P.; Smith, H. E.; Nafie, L. A.; Freedman, T. B.; Zuk, W. M. *J. Chem. Phys.* **1987**, *86*, 1140–1146.
(20) Polavarapu, P. L.; Pickard, S. T.; Smith, H. E.; Black, T. M.; Rauk, A.; Yang, D. *J. Am. Chem. Soc.* **1991**, *113*, 9747–9756.
(21) Shaw, R. A.; Wieser, H.; Dutler, R.; Rauk, A. *J. Am. Chem. Soc.* **1990**, *112*, 5401–5410.
(22) Schurig, V.; Koppenhoefer, B.; Buerkle, W. *J. Org. Chem.* **1980**, *45*, 538–541.
(23) Hatch, L. F.; Nesbitt, S. S. *J. Am. Chem. Soc.* **1950**, *72*, 727–730.
(24) Gao, Y.; Hanson, R. M.; Klunder, J. M.; Ko, S. Y.; Masamune, H.; Sharpless, K. B. *J. Am. Chem. Soc.* **1987**, *109*, 5765–5780.
(25) Grant, B.; Djerassi, C. *J. Org. Chem.* **1974**, *39*, 968–970.
(26) Corey, E. J.; Katzenellenbogen, J. A.; Posner, G. H. *J. Am. Chem. Soc.* **1967**, *89*, 4245–4247.
(27) Hutchins, R. O.; Kandasamy, D.; Maryanoff, C. A.; Masilamani, D.; Maryanoff, B. E. *J. Org. Chem.* **1977**, *42*, 82–91.
(28) van Tamelan, E. E. *J. Am. Chem. Soc.* **1951**, *73*, 3444–3448.

Table II. Theoretical and Experimental Vibrational Properties of (+)-*trans*-(2*R*,3*R*)-Dimethyloxirane (d_0)

expt[a]			theor							
			freq (cm^{-1})		A (km/mol)		$10^{44}R$ (esu^2 cm^2)			group assgnt[b]
freq (cm^{-1})	A (km/mol)	$10^{44}R$ (esu^2 cm^2)	6-31G	6-31G*(0.3)	LMO	VCT	LMO	VCT	sym	6-31G
1489	10.0 (0.3)		1661	1664	0.3	7.6	2.4	16.4	a	H–C*–C*, C*–C*
1455	7.3 (0.3)		1652	1623	8.9	6.7	−19.8	−30.5	b	CH_3
1452	12.4 (0.2)	19.2 (4.9)	1649	1620	16.5	10.3	16.8	22.6	a	CH_3
1441	10.3 (0.4)		1640	1610	8.0	5.7	11.7	24.1	b	CH_3
1420			1622	1603	1.6	0.5	17.5	12.9	a	CH_3, H–C*–C*
1381	18.1 (0.8)	−1.0 (0.6)	1588	1532	15.7	12.1	0.5	4.0	b	CH_3
			1587	1523	0.5	0.0	−3.1	−2.4	a	CH_3
1335	5.6 (1.4)	−3.4 (0.4)	1505	1468	10.9	11.9	−18.8	−21.4	b	H–C*–C*, H–C*–O
1254	2.6 (0.6)	−6.1 (0.5)	1391	1374	0.1	1.4	−2.8	−10.3	a	C*–C*, H–C*–
1163	5.6 (1.8)	11.9 (1.3)	1319	1294	0.1	2.3	2.6	7.7	a	CH_3–C*–H
1154			1307	1278	2.2	2.5	9.6	9.2	b	CH_3–C*–H
1110	16.5 (0.7)	−58.7 (3.3)	1261	1238	7.6	9.3	−47.5	−84.1	a	CH_3–C*–H
			1240	1208	7.9	9.3	−21.3	−1.7	b	CH_3, C–C*
1022	29.5 (0.8)	26.8 (2.4)	1154	1127	16.0	14.2	5.9	25.0	a	CH_3–C*–H
1015			1138	1122	7.2	13.1	−14.9	−56.5	b	C*–C
959	4.2 (0.6)	20.0 (2.7)	1091	1049	6.9	2.9	6.5	10.7	b	CH_3–C*–H
886	18.4 (0.4)	−41.8 (2.7)	956	964	12.4	27.4	−23.9	−50.2	a	C*–C
812	20.2 (0.9)	87.6 (13.7)	866	875	37.2	19.2	35.3	91.3	a	C*–O
722	6.7 (0.2)	38.7 (7.4)	787	804	6.8	11.4	15.4	37.4	b	C*–O

[a] In addition to the bands listed above, the experimental spectra show bands at ~1178, 1075, 780, and 732 cm^{-1}. The weak band at 1178 cm^{-1} contributes to the intensity listed for the 1154- and 1163-cm^{-1} bands. The intensity data presented here are the mean values of four different measurements, two in CCl_4 and two in CS_2 solvent. Values in parentheses are error estimates for the mean values. [b] Major components only.

Table III. Theoretical and Experimental Vibrational Properties of (+)-*trans*-(2*R*,3*R*)-Dimethyloxirane-*2*-d_1 (*2*-d_1)

expt[a]			theor						
			freq (cm^{-1})		A (km/mol)		$10^{44}R$ (esu^2 cm^2)		group assgnt[b]
freq (cm^{-1})	A (km/mol)	$10^{44}R$ (esu^2 cm^2)	6-31G	6-31G*(0.3)	LMO	VCT	LMO	VCT	6-31G
1469	3.2	2.2	1655	1648	3.3	6.0	−3.3	−1.1	CH_3
1451	4.9	−0.4	1651	1622	7.8	5.7	−12.1	−27.2	CH_3
1448	7.5		1647	1619	11.3	10.9	4.0	13.9	CH_3
1443	4.7	5.5	1640	1609	8.4	6.2	10.4	22.2	CH_3
1418	3.1		1607	1599	5.1	2.4	19.9	22.3	H–C*–C*, C*–C*
1379	10.9	−0.5	1588	1529	10.1	8.5	−0.4	4.0	CH_3
			1586	1521	2.9	0.3	−0.9	0.5	CH_3
1296	4.7 (0.1)	−3.7 (0.2)	1446	1424	8.3	11.2	−14.4	−20.2	H–C*–
1150	1.9 (0.01)	6.5 (0.3)	1310	1284	0.9	3.6	9.9	11.2	H–C*–
1131	1.8 (0.1)	−11.2 (0.9)	1278	1243	3.2	2.8	−19.1	−33.9	CH_3
1109	9.0 (0.3)	weak	1224	1207	14.8	16.8	−1.1	3.9	CH_3
1080	12.3 (0.4)	−41.0 (0.9)	1235	1200	6.3	17.0	−16.5	−9.2	CH_3
1064	5.3 (0.2)		1207	1182	10.8	6.8	−30.2	−48.8	C*–C, H–C*–C*
993	1.6 (0.4)	6.8 (0.3)	1126	1099	2.5	1.9	8.2	−2.8	CH_3
922	8.6 (0.2)	−16.8 (0.7)	1012	1000	8.2	15.1	−15.5	−25.9	D–C*–
882	1.1 (0.2)	weak	948	954	7.7	13.5	−7.6	−15.4	D–C*–O, C*–O
872	6.5 (0.6)	−3.0	902	876	1.9	2.0	−4.1	−13.4	D–C*–C*, C*–C
793	13.1	33.5	852	858	39.7	22.6	32.5	90.8	C*–O
719	5.0	23.4	785	800	6.8	11.2	15.4	38.9	C*–O

[a] In addition to the bands listed above, the experimental absorption spectra show bands at 1473, 1331, 1261, 1240, 1018, 806, and 732 cm^{-1}. These are considered to be nonfundamental bands. The intensity data presented here are the mean values of two different measurements, one in CCl_4 and another in CS_2 solvent. Values in parentheses are error estimates for the mean values. [b] Major components only.

to minimize racemization, diethylene glycol was not used as a cosolvent with HMPA.

The experimental and theoretical frequencies, absorption intensities, and rotational strengths are presented in Tables II–IV for the three oxiranes studied here. The vibrational assignments deduced from the ab initio calculations with the 6-31G and 6-31G*(0.3) basis sets are also included in these tables. The experimental data of (+) enantiomers and the theoretical data of (2*R*,3*R*) enantiomers are used in the following discussion.

Each methyl group is expected to have five vibrational modes in the 1600–700-cm^{-1} region. Of these, two are antisymmetric bending modes, one is a symmetric bending mode, and the remaining two are the rocking modes. For dimethyloxirane, therefore, one expects 10 vibrational bands assignable to the CH_3 groups. However some of these will be coupled to H–C*– bending modes in d_0 and *2*-d_1 and may not be purely CH_3 modes. Such coupling would not be present in *2,3*-d_2, and therefore the CH_3 modes may be clearly identified for this molecule. Each methine group is expected to have two bending modes, although these may not be clearly separated from other modes when coupling such as that with the methyl group modes is present. Again in *2,3*-d_2, such coupling is not present, and therefore the bending modes of D–C*– can be isolated. In addition to the aforementioned 14 modes, the 1600–700-cm^{-1} region will contain one C*–C*, two C*–C, and two C*–O stretching modes. The C*–C* stretching mode in *2*-d_1 is not clearly identified due to the mixing with the H–C*– bending motion. The other four stretching modes are clearly identified as summarized in Tables II–IV.

The lowest frequency band in the 1600–700-cm^{-1} region is from the antisymmetric C*–O stretching motion. This band is seen in the experimental spectra (Figures 1 and 2) at 722, 719, and 718 cm^{-1}, respectively, for d_0, *2*-d_1, and *2,3*-d_2. In all three molecules, this mode has positive VCD, and this is correctly reproduced by the LMO–VCD and VCT predictions. It should be noted that in the experimental spectra this band is overlapped by another band, appearing as a shoulder, which is presumed to

Table IV. Theoretical and Experimental Vibrational Properties of (+)-*trans*-(2*R*,3*R*)-Dimethyloxirane-*2,3-d*$_2$ (*2,3-d*$_2$)

expt[a]			theor							
			freq (cm^{-1})		*A* (km/mol)		$10^{44}R$ (esu^2 cm^2)			
freq (cm^{-1})	*A* (km/mol)	$10^{44}R$ (esu^2 cm^2)	6-31G	6-31G*$^{(0.3)}$	LMO	VCT	LMO	VCT	sym	group assgnt[b] 6-31G
1462	4.3	weak	1652	1631	6.4	1.0	9.6	−10.3	a	CH_3 (CH_3, C*–C*)[c]
			1651	1621	7.7	5.5	−20.8	−31.2	b	CH_3
1450	14.6	weak	1644	1617	7.1	11.8	−5.4	−0.2	a	CH_3
	5.2	3.7	1639	1609	9.1	6.7	10.5	22.4	b	CH_3
1403	4.3	1.9	1590	1588	2.2	6.1	1.8	29.1	a	CH_3 (CH_3, C*–C*)[c]
			1587	1527	14.0	7.4	0.8	5.4	b	CH_3
1378	11.1	3.9	1562	1517	2.1	0.2	15.5	6.0	a	C*–C* (CH_3 umbr)[c]
1146	13.8 (0.6)	2.3 (0.9)	1243	1268	15.5	28.2	2.7	−7.2	b	CH_3
1130	2.5 (0.1)	−6.8 (0.6)	1267	1232	1.8	3.6	−21.6	−47.9	a	CH_3
1093	18.6 (1.3)	−15.8 (2.1)	1296	1219	17.9	16.7	−9.9	13.5	a	CH_3
			1231	1195	3.8	3.5	−22.4	−18.6	b	CH_3
1045	2.2 (0.2)	2.9 (1.0)	1187	1158	4.2	3.3	15.8	13.1	b	C*–C
979	6.2 (0.4)	−32.4 (3.6)	1077	1073	5.1	10.0	−33.1	−40.7	a	D–C*–C*
900	3.9 (0.1)	−6.4 (0.9)	984	979	4.7	6.4	−4.5	−19.7	b	D–C*–O
865	9.3 (0.5)	+6.1	938	948	7.3	13.1	1.6	−4.0	a	D–C*–O
802	1.2 (0.0)	weak	911	877	2.2	0.6	−4.5	2.3	b	D–C*–C*
790	weak	weak	897	874	1.4	2.0	−3.2	−22.1	a	C*–C
769	17.7 (1.5)	37.0	833	834	38.6	24.1	29.8	86.9	a	C*–O
718	4.6 (0.1)	38.1 (10.1)	782	798	6.7	11.0	15.5	37.8	b	C*–O

[a] In addition to the bands listed above, the experimental absorption spectrum shows bands at ~1304, 1263, 1240, 1020, and 730 cm^{-1}. These are considered to be nonfundamental bands. The intensity data presented are the mean values of three different measurements, two in CS_2 and one in CCl_4 solvent. Values in parentheses are error estimates for the mean values. [b] Major components only. [c] Prediction by 6-31G*$^{(0.3)}$ force field.

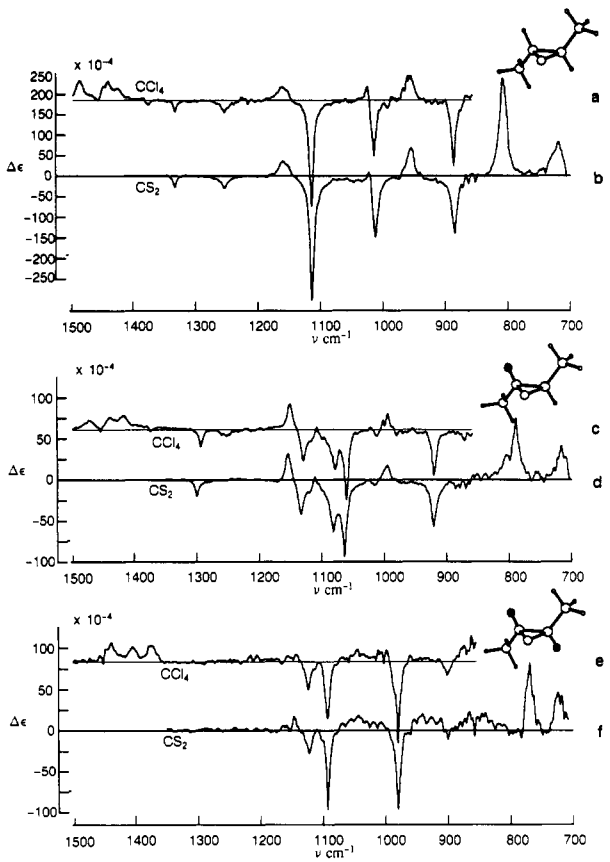

Figure 1. Fourier transform infrared vibrational circular dichroism spectra of (+)-*trans*-2,3-dimethyloxirane (a, b), (+)-*trans*-2,3-dimethyloxirane-*2*-d_1 (c, d), and (+)-*trans*-2,3-dimethyloxirane-*2,3*-d_2 (e, f) in CCl_4 (a, c, e) and CS_2 (b, d, f) solutions: (a) c = 0.34 M, l = 475 μm; (b) c = 0.2 M, l = 540 μm; (c) c = 0.4 M, l = 575 μm; (d) c = 0.4 M, l = 575 μm; (e) c = 0.34 M, l = 525 μm; (f) c = 0.4 M, l = 275 μm.

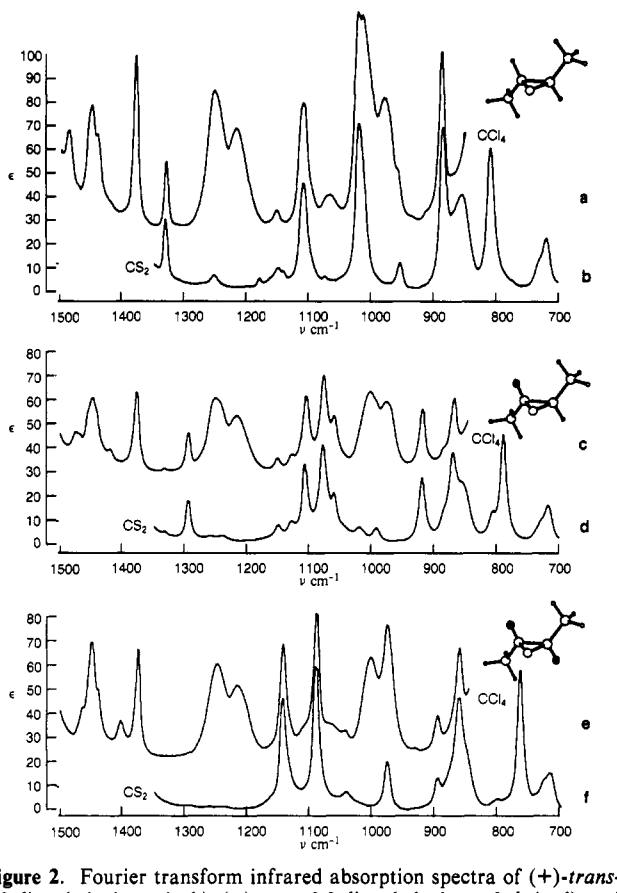

Figure 2. Fourier transform infrared absorption spectra of (+)-*trans*-2,3-dimethyloxirane (a, b), (+)-*trans*-2,3-dimethyloxirane-*2*-d_1 (c, d), and (+)-*trans*-2,3-dimethyloxirane-*2,3*-d_2 (e, f) in CCl_4 (a, c, e) and CS_2 (b, d, f) solutions: (a) c = 0.34 M, l = 475 μm; (b) c = 0.2 M, l = 540 μm; (c) c = 0.4 M, l = 575 μm; (d) c = 0.4 M, l = 575 μm; (e) c = 0.34 M, l = 525 μm; (f) c = 0.4 M, l = 275 μm.

originate from a nonfundamental mode. It is not clear how much this mode contributes to the observed VCD. The entire VCD envelope observed is assumed to come from the C*–O mode. The next band is due to a symmetric C*–O stretching mode which appears at 812, 793, and 769 cm^{-1}, respectively, in the experimental spectra of d_0, *2*-d_1, and *2,3*-d_2. This band also has positive VCD, which again is correctly reproduced by both theoretical methods. In simple theoretical models,[29-31] the two C*–O stretching modes

(29) Holzworth, G.; Chabay, I. *J. Chem. Phys.* **1972**, *57*, 1632–1635.
(30) Nafie, L. A.; Polavarapu, P. L.; Diem, M. *J. Chem. Phys.* **1980**, *73*, 3530–3540.
(31) Polavarapu, P. L. *J. Chem. Phys.* **1987**, *87*, 4419–4422.

would be expected to give bisignate VCD, and the observation of the same VCD sign for both C*–O stretching modes warrants care in applying simple conceptual models for VCD interpretations. Recently, Freedman et al.[32] have predicted weak positive VCD for the C*–O stretching modes of (2*S*,3*S*)-*trans*-2,3-dideuteriooxirane using qualitative arguments. For the corresponding modes of dimethyloxiranes considered here, the observed VCD magnitudes are quite large and are positive for the (2*R*,3*R*) enantiomers. Therefore, their predictions cannot be generalized in any obvious way.

The symmetric C*–C stretching mode appears as the next higher frequency band for all three molecules. This band appears in the experimental spectra at 886, 872, and 790 cm^{-1}, respectively, for d_0, 2-d_1, and 2,3-d_2. The absorption intensity at this band is strong in d_0, medium in 2-d_1, and weak in 2,3-d_2. A strong negative Cotton effect (CE) is observed in d_0, but only a weak negative CE, if any, may be inferred in the VCD spectra of 2-d_1 and 2,3-d_2. These observations are qualitatively reproduced in the theoretical predictions of absorption intensity and VCD for both theoretical models. The decrease in intensities from d_0 to 2-d_1 and to 2,3-d_2 suggests that the coupling of H–C*– bending motions has a strong influence on the observed intensities for the symmetric C*–C stretching mode.

The antisymmetric C*–C stretching mode in d_0 was not clearly identified in a previous experimental study.[1] It could be associated with either of the two overlapping bands at 1015 and 1022 cm^{-1}. On the basis of simple models[31] which predict bisignate VCD for the symmetric and antisymmetric modes, it was thought that since the symmetric C*–C stretching band has negative VCD, the positive VCD associated with the 1022-cm^{-1} band can be regarded as due to the antisymmetric C*–C stretching. However, the antisymmetric C*–C stretching mode in d_0 was unambiguously assigned as the feature at 1015 cm^{-1} on the basis of VCT/6-31G*$^{(0.3)}$ calculations[2] and is reconfirmed by the present LMO–VCD/6-31G calculations. Both ab initio VCD calculations show that both symmetric and antisymmetric C*–C stretching modes have the same negative VCD sign. Thus, once again it appears that the application of simple models for interpreting the observed VCD signs need not give the correct result. On the basis of the 6-31G assignments, this mode is associated with the experimental bands at 1064 and 1045 cm^{-1}, respectively, in 2-d_1 and 2,3-d_2. The 6-31G*$^{(0.3)}$ force field shows the C*–C antisymmetric stretch to be distributed between the three bands at 1109, 1080, and 1064 cm^{-1} in the case of 2-d_1. For 2,3-d_2, the 6-31G*$^{(0.3)}$ force field shows this mode to be strongly mixed with methyl-rocking and ring-breathing modes in each of the experimental bands at 1093 and 1045 cm^{-1} and an unobserved band computed to fall between them. The VCD sign associated with this "mode" is different in these molecules, clearly negative in d_0 and 2-d_1 but having positive and negative components in 2,3-d_2, as seen in the experimental spectra. The sign behavior is reproduced by both theoretical methods but the LMO–VCD/6-31G and VCT/6-31G*$^{(0.3)}$ methods differ in the calculated signs of the transitions at 1109 and 1093 cm^{-1} in 2-d_1 and 2,3-d_2, respectively. The VCT/6-31G*$^{(0.3)}$ result appears to be in error at least in the case of 2,3-d_2.

The C*–C* stretching mode is coupled to the H(D)–C*– bending modes and methyl deformation modes in all three isotopomers. This coupling makes it difficult to identify unambiguously which band has the largest component of C*–C* stretch. In d_0, the C*–C* stretch is distributed principally between the two modes with theoretical frequencies at 1661 and 1391 cm^{-1} (6-31G) or 1664 and 1374 cm^{-1} (6-31G*$^{(0.3)}$). In 2-d_1, the two modes with theoretical frequencies at 1655 and 1607 cm^{-1} (6-31G) or 1648 and 1599 cm^{-1} (6-31G*$^{(0.3)}$) have C*–C* stretching contributions. In 2,3-d_2, this mode is isolated in the 6-31G force field description, the mode with theoretical frequency of 1562 cm^{-1} being implicated. In the 6-31G*$^{(0.3)}$ description, the C*–C* mode is mixed, as in the other isotopomers, the relevant calculated frequencies being 1631 and 1588 cm^{-1}. The 6-31G results suggest that the corresponding experimental band at 1378 cm^{-1} is associated with the C*–C* stretching, while the 6-31G*$^{(0.3)}$ force field identifies this experimental band as due to an umbrella deformation of the methyl groups. In either case, a positive CE is calculated and observed at this position. In d_0, the corresponding band at 1254 cm^{-1} has negative VCD, and in 2,3-d_2, the bands at 1378 and 1403 cm^{-1} have positive VCD. Both theoretical predictions replicate these signs.

In 2,3-d_2, four D–C*– bending modes can be identified. These have theoretical frequencies 1077, 984, 938, and 911 cm^{-1} (6-31G) and 1073, 979, 948, and 877 cm^{-1} (6-31G*$^{(0.3)}$). In simple theoretical models,[29-31] one would have expected to see two bisignate couplets associated with these modes. However, the LMO–VCD predictions indicate that three of these modes have negative signs and only one mode at 938 cm^{-1} has a positive sign. The predictions obtained for the first three modes agree with the experimental observations for the corresponding bands at 979, 900, and 865 cm^{-1}. The experimental VCD band at 802 cm^{-1} is very weak, and therefore the sign associated with the fourth mode cannot be verified. Similar observations are obtained for the VCT/6-31G*$^{(0.3)}$ method, except that the sign associated with the VCD band at 865 cm^{-1} is erroneously reversed. In 2-d_1, two D–C*– bending modes with the 6-31G theoretical frequencies 1012 and 948 cm^{-1} correspond to the experimental bands at 922 and 882 cm^{-1}. Both modes are predicted to have negative VCD signs. In the experimental spectrum, the band corresponding to the higher frequency mode has a negative sign, confirming the theoretical predictions. The second experimental band at 882 cm^{-1} is very weak. In contrast to the D–C*– bending modes, the H–C*– bending modes of 2-d_1 with theoretical frequencies 1446 and 1310 cm^{-1} have bisignate VCD signs and are in agreement with the experimental observations for the corresponding bands at 1296 and 1150 cm^{-1}. The ubiquitous coupling between H–C*– and CH_3 bending motions may have some contribution to the observed couplet. In d_0, as mentioned earlier, the coupling between H–C*– and CH_3 bending motions makes it difficult to identify the modes that are solely from H–C*– bending motions. Two of the H–C*– bending modes identified earlier with the experimental bands at 1489 and 1335 cm^{-1} do exhibit bisignate VCD bands, as predicted both by ab initio theories and by the simple model predictions. However, the failure to see such bisignate features for several other cases (vide supra) makes the agreement obtained for simple model predictions somewhat fortuitous.

For the CH_3 bending modes, there are some consistent patterns in the three molecules studied. First, the symmetric CH_3 bending (umbrella) motions of the two CH_3 groups give rise to nearly degenerate bands at 1381, 1379, and 1403 cm^{-1}, respectively, in d_0, 2-d_1, and 2,3-d_2. In all three cases, the associated VCD is very small. Second, four high-frequency CH_3 bending modes give rise to a negative–positive VCD couplet in the LMO–VCD predictions. This couplet is apparent in d_0, with the experimental bands at 1455, 1452, 1441, and 1420 cm^{-1}. In 2-d_1, this couplet is reversed in signs with the experimental bands at 1469, 1451, and 1448 cm^{-1}, suggesting that the predicted frequency ordering of modes may be in question. In 2,3-d_2, the negative–positive couplet is apparent, with the negative portion appearing as very weak at 1462 cm^{-1} and the positive portion showing clearly at 1450 cm^{-1}. Although a single CH_3 group is unlikely to give rise to significant VCD associated with the antisymmetric CH_3 bending modes, as evidenced in the VCD spectra of methyloxirane and methylthiirane, the dimethyloxiranes studied here indicate that a linear combination of two CH_3 modes may give significant and characteristic VCD sign patterns.

The CH_3 rocking modes show some very interesting VCD features. In 2,3-d_2, the 1146-cm^{-1} experimental band is associated with the theoretical mode at 1243 cm^{-1}, due to stronger absorption intensity and weak positive VCD associated with them. The 1130-cm^{-1} experimental band and the 1267-cm^{-1} theoretical mode are associated with weak absorption intensity but fairly large negative VCD. Although a small absorption intensity is obtained through simulation for the experimental band at 1130 cm^{-1}, there is no visible trace of this band in the experimental absorption

(32) Freedman, T. B.; Spencer, K. M.; Ragunathan, N.; Nafie, L. A.; Moore, J. A.; Schwaab, J. M. *Can. J. Chem.* **1991**, *69*, 1619.

spectrum. Therefore the experimental VCD band at 1130 cm^{-1} has a very large dissymmetry factor. The third rocking mode associated with the experimental band at 1093 cm^{-1} and the theoretical mode at 1296 cm^{-1} has fairly strong absorption and negative VCD. The fourth rocking mode is probably also associated with the experimental band at 1093 cm^{-1}, since a separate band corresponding to the theoretical mode at 1231 cm^{-1} is not seen. In *2-d_1*, the CH_3 rocking modes have features similar to those in *2,3-d_2*. Three of them, with experimental frequencies 1131, 1109, and 1080 cm^{-1}, have negative VCD, and the fourth one, at 993 cm^{-1}, has positive VCD. The 1131-cm^{-1} band has very weak absorption but large negative VCD, thereby yielding a large dissymmetry factor, just like the 1130-cm^{-1} band of *2,3-d_2*. The signs predicted for the theoretical modes at 1278, 1224, 1235, and 1126 cm^{-1} are in agreement with those observed for the corresponding experimental bands. In d_0, the CH_3 rocking modes are mixed with the H–C*– bending modes and the experimental bands at 1163, 1154, 1110, 1022, and 959 cm^{-1} are associated with theoretical modes that have contributions from the CH_3 groups. Therefore it is not easy to correlate the CH_3 rocking modes of d_1 and 2,3-d_2 with those of d_0.

Experimental and Computational Details

Melting points were taken in open capillary tubes and are corrected. Boiling points are uncorrected. Rotatory powers at the sodium line were measured with an Autopol III automatic polarimeter and a 1-dm sample tube unless otherwise noted. Proton magnetic resonance (^1H NMR) spectra were obtained in chloroform-*d* with tetramethylsilane as an internal standard on a JEOL JNM-FX 90Q or Bruker AM-300 spectrometer operating at 90 or 300 MHz, respectively. Chemical shifts (δ) are reported in parts per million (ppm) downfield from the standard.

***trans*-2-Buten-1-ol (2a).** A dry, 500-mL, three-necked flask was charged with dry tetrahydrofuran (300 mL), flushed with nitrogen, and then cooled in ice. Lithium aluminum hydride (13.8 g, 0.364 mol) was added, and the mixture was stirred for 15–20 min. 2-Butyn-1-ol (**1**) (25.0 g, 0.357 mol) was added dropwise, during which hydrogen gas was evolved. The reaction mixture was stirred at room temperature for 18–20 h; then the reaction was cooled to −20 °C and quenched by the careful dropwise addition of water (27 g, 1.5 mol) with stirring over about 30 min. The mixture was gradually allowed to warm to room temperature, and after 1–2 h, the flask was vigorously swirled to break up the cake of inorganic salts. The mixture was poured over ice (100 g), and sufficient 6 N hydrochloric acid was added to dissolve most of the aluminum hydroxide. The resulting aqueous solution was extracted with methylene chloride (2 × 100 mL). The organic layer was dried (Na_2SO_4), and the solvent was removed through a distilling column. Distillation of the residue gave **2a** (14.2 g, 55%): bp 118–122 °C [lit.[23] bp 121.2 °C (754 mmHg)]; ^1H NMR (90 MHz) δ 1.46 (b s, 1, OH), 1.72 (d, 3, J = 3.6 Hz, CH_3), 4.05 (b s, 2, CH_2), 5.76 ppm (m, 2, CH=CH).

***trans*-2-Buten-1-ol-*2,3-d*$_2$ (2b)** was prepared (65%) from **1** as described above for **2a** except that the lithium aluminum deuteride was used in place of lithium aluminum hydride and deuterium oxide was used in place of water to quench the reaction: bp 119–121 °C; ^1H NMR (300 MHz) δ 1.66 (s, 3, CH_3), 1.84 (b s, 1, OH), 4.01 ppm (s, 2, CH_2).

***trans*-2-Buten-1-ol-*3-d* (2c)** was prepared (61%) from **1** as described above for **2a** except that deuterium oxide was used in place of water to quench the reaction: bp 119–121 °C; ^1H NMR (300 MHz) δ 1.71 (s, 3, CH_3), 1.79 (s, 1, OH), 4.06 (dd, 2, J = 1.0 and 6.0 Hz, CH_2), 5.65 ppm (m, 1, CH).

(2*S*,3*S*)-2-(Hydroxymethyl)-3-methyloxirane [(2*S*,3*S*)-3a] was prepared using a slight modification of a procedure used by Sharpless.[24] Thus, crushed, activated 4-Å molecular sieves (5 g) were introduced into a carefully dried, 500-mL, three-necked flask equipped with an addition funnel. Methylene chloride (250 mL) was added, and the flask was flushed with nitrogen for several minutes and then cooled to about −20 °C. Diethyl L-(+)-tartrate (1.2 g, 5.8 mmol), titanium isopropoxide (1.4 g, 4.9 mmol), and *trans*-2-buten-1-ol (**2a**) (7.21 g, 0.100 mmol) were sequentially added with stirring. The alcohol was first dissolved in methylene chloride (10 mL), and this solution was dried for 20 min over crushed 4-Å molecular sieves before addition. Stirring was continued at −20 °C for 15–20 min, and then 5.3 M *tert*-butyl hydroperoxide (28 mL, 0.15 mol) in isooctane, dried over crushed 4-Å molecular sieves for 20 min, was added dropwise to the mixture. The reaction mixture was then transferred to the freezer (−15 °C) and stored overnight, after which it was returned to the cooling bath at −20 °C. The reaction was quenched by the slow addition of triphenylphosphine (13.1 g, 49.9 mmol), followed by a solution of citric acid monohydrate (1.05 g, 5.00 mmol) in acetone (20 mL); the temperature of the reaction mixture was kept below −10 °C during the additions. The cooling bath was removed, and the reaction mixture was filtered and evaporated to a volume of about 75 mL. Ether (100 mL) was added with swirling, whereupon a white precipitate formed. The latter was removed by filtration, and the filtrate was evaporated to a residual oil. Distillation of the residue gave (2*S*,3*S*)-**3a** (4.85 g, 55%, chemical purity about 90% from its ^1H NMR spectrum): bp 65–68 °C (15 mmHg); $[\alpha]^{25}_D$ −48° (*c* 1.6, C_6H_6) [lit.[24] $[\alpha]^{25}_D$ −50.1° (*c* 4.54, C_6H_6) for 93% chemical purity, 90–92% ee], 90% ee; ^1H NMR (90 MHz) δ 1.28 (d, 3, J = 5.3 Hz, CH_3), 2.60 (b s, 1, OH), 2.82 (m, 1, CH), 2.99 (dq, 1, J = 2.6 and 5.3 Hz, OCH), 3.54 (dd, 1, J = 4.4 and 12.7 Hz, *H*CH), 3.81 ppm (dd, 1, J = 2.9 and 12.5 Hz, HC*H*).

(2*S*,3*S*)-2-(Hydroxymethyl)-3-methyloxirane-*2,3-d*$_2$ [(2*S*,3*S*)-3b] was prepared (43%, chemical purity about 95% from its ^1H NMR spectrum) from *trans*-2-buten-1-ol-*2,3-d*$_2$ (**2b**) as described above for the preparation of (2*S*,3*S*)-**3a** from **2a**: bp 65–68 °C (15 mmHg); $[\alpha]^{25}_D$ −51° (*c* 2.68, C_6H_6); ^1H NMR (90 MHz) δ 1.33 (s, 3, CH_3), 2.26 (b s, 1, OH), 3.62 (d, 1, J = 12.8 Hz, *H*CH), 3.87 ppm (d, 1, J = 12.8 Hz, HC*H*).

(2*R*,3*R*)-2-(Hydroxymethyl)-3-methyloxirane-*2,3-d*$_2$ [(2*R*,3*R*)-3b] was prepared (43%, chemical purity about 85% from its ^1H NMR spectrum) from *trans*-2-buten-1-ol-*2,3-d*$_2$ (**2b**) as described above for the preparation of (2*S*,3*S*)-**3a** from **2a** except that diethyl D-(−)-tartrate was used in place of diethyl L-(+)-tartrate: bp 65–68 °C (15 mmHg); $[\alpha]^{25}_D$ +48° (*c* 2.47, C_6H_6); ^1H NMR (90 MHz) identical to that of (2*S*,3*S*)-**3b**.

(2*S*,3*S*)-2-(Hydroxymethyl)-3-methyloxirane-*3-d* [(2*S*,3*S*)-3c] was prepared (52%) from *trans*-2-buten-1-ol-*3-d* (**2c**) as described above for the preparation of (2*S*,3*S*)-**3a** from **2a**: bp 69–72 °C (15 mmHg); $[\alpha]^{25}_D$ −54° (*c* 1.45, C_6H_6); ^1H NMR (90 MHz) δ 1.34 (s, 3, CH_3), 2.07 (b s, 1, OH), 2.88 (dd, 1, J = 2.6 and 4.4 Hz, CH), 3.60 (dd, 1, J = 4.0 and 11.9 Hz, *H*CH), 3.91 ppm (dd, 1, J = 2.5 and 12 Hz, HC*H*). A small doublet in the ^1H NMR spectrum at 1.35 ppm and a small quartet at 3.0 ppm indicated that there was about 15–20% 2-(hydroxymethyl)-3-methyloxirane-*2-d* present. Otherwise the chemical purity of (2*S*,3*S*)-**3c** appeared to be greater than 95%.

(2*R*,3*R*)-2-(Hydroxymethyl)-3-methyloxirane-*3-d* [(2*R*,3*R*)-3c] was prepared (47%) from *trans*-2-buten-1-ol-*3-d* (**2c**) as described above for the preparation of (2*S*,3*S*)-**3a** from **2a** except that diethyl D-(−)-tartrate was used in place of diethyl L-(+)-tartrate: bp 69–72 °C (15 mmHg); $[\alpha]^{25}_D$ +50° (*c* 1.1, C_6H_6); ^1H NMR (90 MHz) identical to that of (2*S*,3*S*)-**3c**, also showing 15–20% contamination with 2-(hydroxymethyl)-3-methyloxirane-*2-d*.

(2*S*,3*S*)-2-(Hydroxymethyl)-3-methyl-*O*-((*p*-nitrophenyl)sulfonyl)-oxirane [(2*S*,3*S*)-4a]. Diisopropylamine (6.3 g, 0.062 mol) and (2*S*,3*S*)-2-(hydroxymethyl)-3-methyloxirane [(2*S*,3*S*)-**3a**] (5.0 g, 0.057 mol) were dissolved in methylene chloride (50 mL), and the solution was cooled in an ice bath. While the solution stirred, *p*-nitrobenzenesulfonyl chloride (13.8 g, 66.5 mmol), freshly recrystallized from ether, was added in portions. The reaction mixture was kept in the ice bath for 20 min and then allowed to stir at room temperature for an additional 1–2 h, during which time diisopropylamine hydrochloride crystallized. It was removed by filtration, and the reaction mixture was washed with 1 N sulfuric acid (2 × 50 mL) and then dried ($MgSO_4$). The methylene chloride solution was filtered through a short silica gel (20 g) column, using additional methylene chloride to elute the reaction product completely from the silica gel. Evaporation of the methylene chloride gave an orange solid. Recrytallization of this solid from a minimum of ether–methylene chloride gave (2*S*,3*S*)-**4a** (7.8 g, 50%) as a white crystalline solid: mp 70–80 °C, $[\alpha]^{25}_D$ −34° (*c* 2.03, $CHCl_3$); ^1H NMR (90 MHz) δ 1.31 (d, 3, J = 4.8 Hz, CH_3), 2.95 (m, 2, HCCH), 4.04 (dd, 1, J = 6.2 and 11.4 Hz, *H*CH), 4.42 (dd, 1, J = 3.1 and 11.4 Hz, HC*H*), 8.13 (d, 2, J = 8.8 Hz, aromatic H), 8.41 ppm (d, 2, J = 9.2 Hz, aromatic H).

(2*S*,3*S*)-2-(Hydroxymethyl)-3-methyl-*O*-((*p*-nitrophenyl)sulfonyl)-oxirane-*2,3-d*$_2$ [(2*S*,3*S*)-4b] was prepared (65%) from (2*S*,3*S*)-2-(hydroxymethyl)-3-methyloxirane-*2,3-d*$_2$ [(2*S*,3*S*)-**3b**] as described above for the preparation of (2*S*,3*S*)-**4a** from (2*S*,3*S*)-**3a**: mp 65–74 °C; $[\alpha]^{25}_D$ −34° (*c* 2.5, $CHCl_3$); ^1H NMR (90 MHz) δ 1.31 (s, 3, CH_3), 4.06 (d, 1, J = 11.4 Hz, *H*CH), 4.39 (d, 1, J = 11.4 Hz, HC*H*), 8.13 (d, 2, J = 9.2 Hz, aromatic H), 8.40 ppm (d, 2, J = 9.2 Hz, aromatic H).

(2*R*,3*R*)-2-(Hydroxymethyl)-3-methyl-*O*-((*p*-nitrophenyl)sulfonyl)-oxirane-*2,3-d*$_2$ [(2*R*,3*R*)-4b] was prepared (65%) from (2*R*,3*R*)-2-(hydroxymethyl)-3-methyloxirane-*2,3-d*$_2$ [(2*R*,3*R*)-**3b**] as described above for the preparation of (2*S*,3*S*)-**4a** from (2*S*,3*S*)-**3a**: mp 68–74 °C; $[\alpha]^{25}_D$ +35° (*c* 2.5, $CHCl_3$); ^1H NMR (90 MHz) identical to that of (2*S*,3*S*)-**4b**.

(2*S*,3*S*)-2-(Hydroxymethyl)-3-methyl-*O*-((*p*-nitrophenyl)sulfonyl)-oxirane-*3-d* [(2*S*,3*S*)-4c] was prepared (65%) from (2*S*,3*S*)-2-(hydroxymethyl)-3-methyloxirane-*3-d* [(2*S*,3*S*)-**3c**] as described above for the preparation of (2*S*,3*S*)-**4a** from (2*S*,3*S*)-**3a**: mp 66–75 °C; $[\alpha]^{25}_D$ −35°

(c 3.65, $CHCl_3$); ^1H NMR (300 MHz) δ 1.31 (s, 3, CH_3), 2.95 (dd, 1, J = 3.2 and 6.3 Hz, CH), 4.05 (dd, 1, J = 6.3 and 11.4 Hz, HCH), 4.41 (dd, 1, J = 3.1 and 11.5 Hz, HCH), 8.13 (d, 2, J = 7.0 Hz, aromatic H), 8.41 ppm (d, 2, J = 7.1 Hz, aromatic H).

(2R,3R)-2-(Hydroxymethyl)-3-methyl-O-((p-nitrophenyl)sulfonyl)-oxirane-3-d [(2R,3R)-4c] was prepared (68%) from (2R,3R)-2-(hydroxymethyl)-3-methyloxirane-3-d [(2R,3R)-3c] as described above for the preparation of (2S,3S)-4a from (2S,3S)-3a: mp 65–72 °C; ^1H NMR (300 MHz) identical to that of (2S,3S)-4c.

(2S,3S)-2,3-Dimethyloxirane [(2S,3S)-5a]. A 250-mL round-bottomed flask was charged with hexamethylphosphoramide (HMPA) (50 mL) and finely divided sodium cyanoborohydride (8.3 g, 0.13 mol). The stirred mixture was warmed to 40–50 °C for about 30 min. The temperature was then increased until it reached about 70 °C, at which time (2S,3S)-2-(hydroxymethyl)-3-methyl-O-((p-nitrophenyl)sulfonyl)oxirane [(2S,3S)-4a] (14.5 g, 53.1 mmol) was added. A small distilling head with a vacuum takeoff, previously assembled, was quickly attached, and reduced pressure (water pump) was applied as the heating was continued. The reaction mixture boiled as the product was formed and distilled. The distillate was collected in a dry ice-cooled receiver. The reaction was exothermic, and as the reaction mixture began to boil vigorously, the external heat was removed. The reaction was complete in 10–15 min. Redistillation of the crude product from sodium hydroxide pellets gave pure (2S,3S)-5a (1.5 g, 39%): bp 54–56 °C (collect up to 56 °C in an ice-cooled receiver); $[\alpha]^{25}_D$ −19.6° (neat, 0.5 dm) [lit.[22] $[\alpha]^{25}_D$ −47.02° (neat, 1 dm), 100% ee], 83% ee; ^1H NMR (90 MHz) δ 1.29 (d, 6, J = 4.8 Hz, CH_3), 2.71 ppm (q, 2, J = 4.6 Hz, CH).

(2S,3S)-2,3-Dimethyloxirane-2,3-d_2 [(2S,3S)-5b] was prepared (20%) from (2S,3S)-2-(hydroxymethyl)-3-methyl-O-((p-nitrophenyl)-sulfonyl)oxirane-2,3-d_2 [(2S,3S)-4b] as described above for the preparation of (2S,3S)-5a from (2S,3S)-4a: bp 54–56 °C; $[\alpha]^{23}_D$ −19.5° (neat, 0.5 dm), 80% ee based on the rotatory power of its enantiomer, (2R,3R)-5b, for which the ee was determined using the chiral shift reagent[33] Eu(tcf)$_3$ during observation of its 300-MHz ^1H NMR spectrum: ^1H NMR (90 MHz) δ 1.28 ppm (s, CH_3).

(2R,3R)-2,3-Dimethyloxirane-2,3-d_2 [(2R,3R)-5b] was prepared (40%) from (2R,3R)-2-(hydroxymethyl)-3-methyl-O-((p-nitrophenyl)-sulfonyl)oxirane-2,3-d_2 [(2R,3R)-4b] as described above for the preparation of (2S,3S)-5a from (2S,3S)-4a: bp 54–56 °C; $[\alpha]^{25}_D$ +18.1° (neat, 0.5 dm), 75% ee determined using the chiral shift reagent[33] Eu(tcf)$_3$ during observation of its 300-MHz ^1H NMR spectrum; ^1H NMR (90 MHz) identical to that of (2S,3S)-5b.

(2S,3S)-2,3-Dimethyloxirane-2-d [(2S,3S)-5c] was prepared (29%) from (2S,3S)-2-(hydroxymethyl)-3-methyl-O-((p-nitrophenyl)sulfonyl)-oxirane-2-d_2 [(2S,3S)-4c] as described above for the preparation of (2S,3S)-5a from (2S,3S)-4a: bp 54–56 °C; $[\alpha]^{25}_D$ −19.2° (neat, 0.5 dm), 85% ee determined using the chiral shift reagent[33] Eu(tcf)$_3$ during observation of its 300-MHz ^1H NMR spectrum; ^1H NMR (90 MHz) δ 1.28 (d, 3, J = 4.8 Hz, CH_3), 1.28 (s, 3, CH_3), 2.71 ppm (q, 1, J = 5.3 Hz, CH).

(2R,3R)-2,3-Dimethyloxirane-2-d [(2R,3R)-5c] was prepared (14%) from (2R,3R)-2-(hydroxymethyl)-3-methyl-O-((p-nitrophenyl)-sulfonyl)oxirane-2-d_2 [(2R,3R)-4c] as described above for the preparation of (2S,3S)-5a from (2S,3S)-4a: bp 54–56 °C; $[\alpha]^{25}_D$ +19.0° (neat, 0.5 dm), 85% ee based on the rotatory power of its enantiomer, (2S,3S)-5c, for which the ee was determined using the chiral shift reagent[33] Eu(tcf)$_3$ during observation of its 300-MHz ^1H NMR spectrum; ^1H NMR (90 MHz) identical to that of (2S,3S)-5c.

Determination of Enantiomeric Excess. Approximately 15 mg of the oxirane and 38 mg of the chiral lanthanide shift reagent tris[3-((trifluoromethyl)hydroxymethylene)-(+)-camphorato]europium(III) [Eu(tfc)$_3$] were added to an NMR sample tube containing benzene-d_6 (0.50–0.75 mL), and the mixture was allowed to stand overnight. In the 300-MHz ^1H NMR spectrum of this solution, the methyl signals of the two diastereomeric oxirane complexes absorbed at about 2.5 ppm downfield from TMS and were separated by about 0.1 ppm (30 Hz). The signals were slightly overlapped, and their relative areas were determined by triangulation. The reported enantiomeric excesses (ee's) have been rounded to the nearest 5% and are probably accurate to about ±5%.

VCD spectra in the 1600–700-cm^{-1} region were measured at 4-cm^{-1} resolution on an instrument built at Vanderbilt.[34] A liquid nitrogen-cooled HgCdTe detector (D^* = 4 × 10^{10}, 600-cm^{-1} cutoff), ZnSe photoelastic modulator, and KRS-5 polarizer were used. The base-line artifacts were minimized by taking half of the difference between the raw VCD of the (+) and (−) enantiomers. The experimental rotational strengths, R, were determined from the frequency-weighted integrated areas as

$$R = \frac{0.23 \times 10^{-38}}{cl} \int \frac{\Delta A(\nu)}{\nu} \, d\nu \approx \frac{0.23 \times 10^{-38}}{cl\nu_0} \int \Delta A(\nu) \, d\nu$$

where c is concentration, l is the path length, ν_0 is the band center, and $\Delta A(\nu) = A_L(\nu) - A_R(\nu)$ with $A_L(\nu)$ and $A_R(\nu)$ representing respectively the absorbance for left and right circularly polarized light at frequency ν. In cases where two or more bands overlap, the combined rotational strength is reported. The observed rotational strengths are corrected for enantiomeric excess so that tabulated values correspond to pure enantiomers. The experimental absorption intensities were determined by fitting of Lorentzian curves to the experimental IR spectra after subtracting the solvent absorption. Due to the arbitrariness in the curve-fitting procedure, the absorption intensities determined by the curve-fitting procedure are somewhat approximate. To provide error estimates in the measured values, the mean values from different independent measurements and the associated standard deviations are presented.

LMO–VCD Method. In the localized molecular orbital (LMO–VCD) method,[7–9] the expression of rotational strength for a vibrational normal mode j is given as

$$R_j = \frac{e^2\hbar}{4c}[\{\sum_{n=1}^{n_{nuclei}} \xi_n \mathbf{s}_n^j - \sum_{i=1}^{n_{electrons}} \sigma_i^j\} \cdot \{\sum_{n=1}^{n_{nuclei}} \xi_n(\mathbf{R}_n \times \mathbf{s}_n^j) - \sum_{i=1}^{n_{electrons}} \mathbf{r}_i^0 \times \sigma_i^j\}] \quad (1)$$

where ξ_n is the bare nuclear charge of atom n with positional vector $\mathbf{R}_n$ and displacement vector $\mathbf{s}_n^j = (\partial \mathbf{R}_n/\partial Q_j)$ during a normal vibrational mode Q_j, $\mathbf{r}_i^0$ is the centroid of the localized molecular orbital occupied by the ith electron, and $\sigma_i^j = (\partial \mathbf{r}_i/\partial Q_j)$ is the displacement of the orbital centroid during vibration j.

VCT Method. In the vibronic coupling theoretical (VCT) method of Nafie and Freedman,[6] the individual electric and magnetic dipole transition moments become respectively

$$\mu^{VC}_{(00,01)j} = e\left(\frac{\hbar}{2\omega_j}\right)^{1/2}\left[\sum_{n=1}^{n_{atoms}} \xi_n \mathbf{s}_n^j - 2\sum_{n=1}^{n_{atoms}}\sum_{i=1}^{n_{electrons}}\sum_{e=1}^{n_{ex}} \langle\Psi_0|\mathbf{r}_i|\Psi_e\rangle\left\langle\Psi_e\left|\frac{\partial}{\partial \mathbf{R}_n}\right|\Psi_0\right\rangle \mathbf{s}_n^j\right] \quad (2.1)$$

$$= e\left(\frac{\hbar}{2\omega_j}\right)^{1/2}\left[\sum_{n=1}^{n_{atoms}} \xi_n \mathbf{s}_n^j - 2\sum_{n=1}^{n_{atoms}}\sum_{i=1}^{n_{electrons}} \left\langle\Psi_0\left|\mathbf{r}_i\frac{\partial}{\partial \mathbf{R}_n}\right|\Psi_0\right\rangle \mathbf{s}_n^j\right] \quad (2.2)$$

and

$$\mathbf{m}^{VC}_{(00,01)j} = \frac{e}{2c}\left(\frac{\hbar\omega_j}{2}\right)^{1/2}\left[i\sum_{n=1}^{n_{atoms}} \xi_n(\mathbf{R}_n \times \mathbf{s}_n^j) - 2\sum_{n=1}^{n_{atoms}}\sum_{i=1}^{n_{electrons}}\sum_{e=1}^{n_{ex}} \langle\Psi_0|\mathbf{r}_i \times \mathbf{p}_i|\Psi_e\rangle\left\langle\Psi_e\left|\frac{\partial}{\partial \mathbf{R}_n}\right|\Psi_0\right\rangle \mathbf{s}_n^j \frac{1}{E_e^0 - E_0^0}\right] \quad (3)$$

where $\mathbf{r}_i$ and $\mathbf{p}_i$ are the position and momentum of the ith electron, ω_j is the frequency of the jth normal mode, and $E_e^0 - E_0^0$ is the vertical electronic excitation energy. The electronic wavefunctions are denoted by Ψ_0 and Ψ_e. The energy difference and all matrix elements are evaluated at the equilibrium geometry of the ground state. The superscript VC denotes that these expressions describe a vibronic coupling mechanism for IR and VCD intensities. The subscript (00,01) signifies that the transition is between the ν = 0 and ν = 1 vibrational levels of the ground electronic state of the molecule. The VCT rotational strength is the imaginary part of the scalar product of $\mu^{VC}_{(00,01)j}$ and $\mathbf{m}^{VC}_{(00,01)j}$.

Ab initio calculations were done with 6-31G and 6-31G*$^{(0.3)}$ basis sets at the corresponding optimized geometries. The 6-31G*$^{(0.3)}$ basis set[2] is a modification of the internal 6-31G* basis set of GAUSSIAN 86[35] (and its antecedents) which is particularly suitable for VCD intensities by the Dutler and Rauk implementation[11] of VCT.[6] The VCT intensities, which are evaluated in a common origin gauge with the origin at the molecular center of mass, were obtained using the program FREQ86[36] with the 6-

(33) McCreary, M. D.; Lewis, D. W.; Wernick, D. L.; Whitesides, G. M. *J. Am. Chem. Soc.* **1974**, *96*, 1038–1054.

(34) Polavarapu, P. L. *Appl. Spectrosc.* **1989**, *43*, 1295–1297.

(35) Frisch, M. J.; Binkley, J. S.; Schlegel, H. B.; Raghavachari, K.; Melius, C. F.; Martin, L. R.; Stewart, J. J. P.; Bobrowicz, F. W.; Rohlfing, C. M.; Kahn, L. R.; De Frees, D. J.; Seeger, R.; Whiteside, R. A.; Fox, D. J.; Fleuder, E. M.; Pople, J. A. GAUSSIAN 86; Carnegie-Mellon Publishing Unit: Pittsburgh, PA, 1986. The version at the University of Calgary was modified to write Fock and overlap matrix derivatives to the read–write file for VCD calculations.

(36) FREQ86: a version of FREQ85[11] modified to be compatible with GAUSSIAN 86.[35]

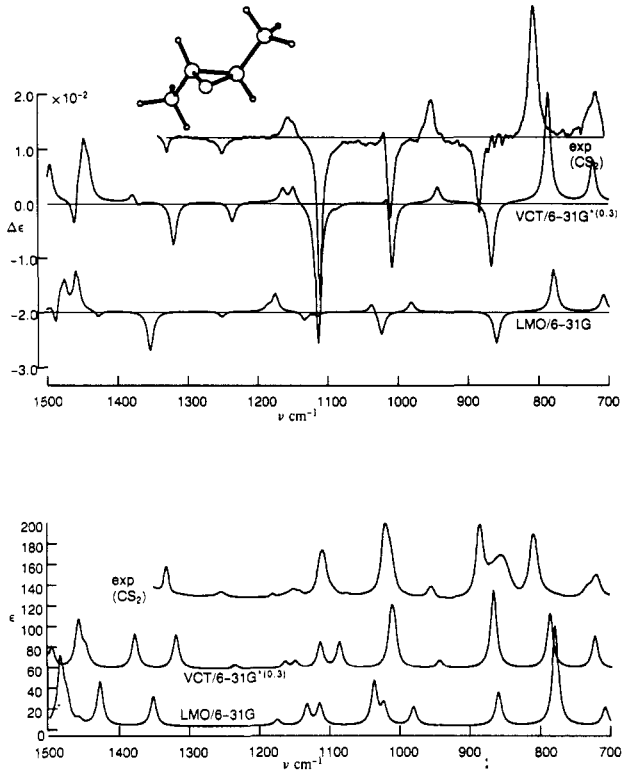

Figure 3. Theoretical and experimental VCD and IR spectra of (+)-*trans*-2,3-dimethyloxirane.

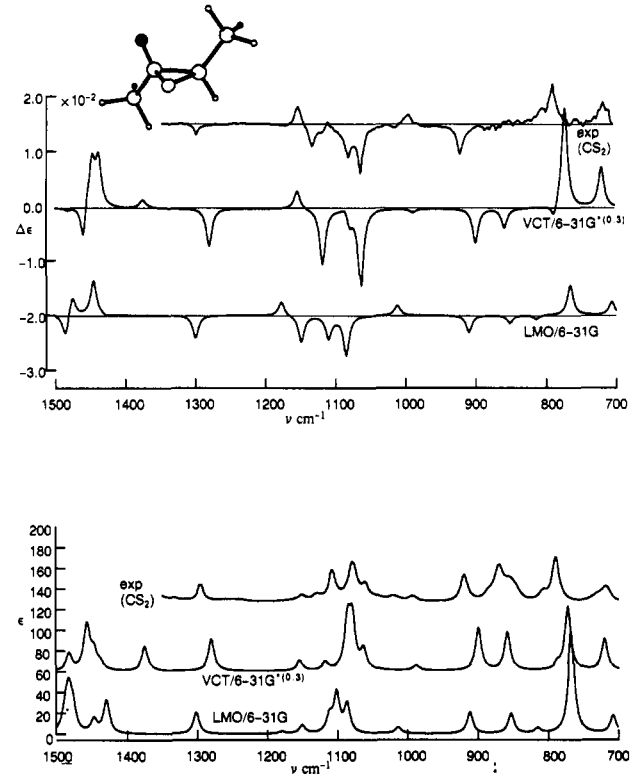

Figure 4. Theoretical and experimental VCD and IR spectra of (+)-*trans*-2,3-dimethyloxirane-2-d_1.

31G*(0.3) basis set (VCT/6-31G*(0.3)). VCD intensities were also calculated by using the LMO–VCD method[7-9] with the 6-31G basis set (LMO–VCD/6-31G). The localized molecular orbitals were obtained through Boys' localization scheme,[37] as implemented in the GAMESS program.[38] The derivatives of orbital centroids required to obtain the magnetic dipole moment derivatives were obtained numerically by displacing the nuclei by 0.005 Å. The absorption intensities obtained from the orbital centroids and their nuclear displacement derivatives were equal (within numerical errors) to those obtained using analytical methods. This criterion and the sum rules[39] were used to verify the LMO–VCD program that was developed for these calculations.

The theoretical results are displayed as simulated spectra using Lorentzian line shapes each with a 10-cm^{-1} band width (full width at half-height) in Figures 3–5. The ab initio harmonic frequencies were uniformly scaled by 0.9 to compensate for systematic errors in the computation of force constants at the Hartree–Fock level[40] and to make comparison with the experimental spectra easier. Such systematic errors can be reduced by going to higher levels of theory such as the MP2 method, but they are not pursued here due to computational limitations.

Conclusions

The syntheses of both enantiomers of *trans*-2,3-dimethyloxirane-d_0, *trans*-2,3-dimethyloxirane-2-d_1, and *trans*-2,3-dimethyloxirane-2,3-d_2 have been described. Vibrational circular dichroism (VCD) spectra for these compounds were obtained in the 1600–700-cm^{-1} region and compared with the results of ab initio theoretical calculations using the localized molecular orbital method (LMO–VCD) and the vibronic coupling theoretical method (VCT). Both theories produce theoretical VCD predictions which are in very satisfactory agreement with the experimental spectra, permitting a detailed assignment of the vibrational modes. More importantly, in present and earlier studies indicate that absolute configurations can be confidently determined using vibrational circular dichroism.

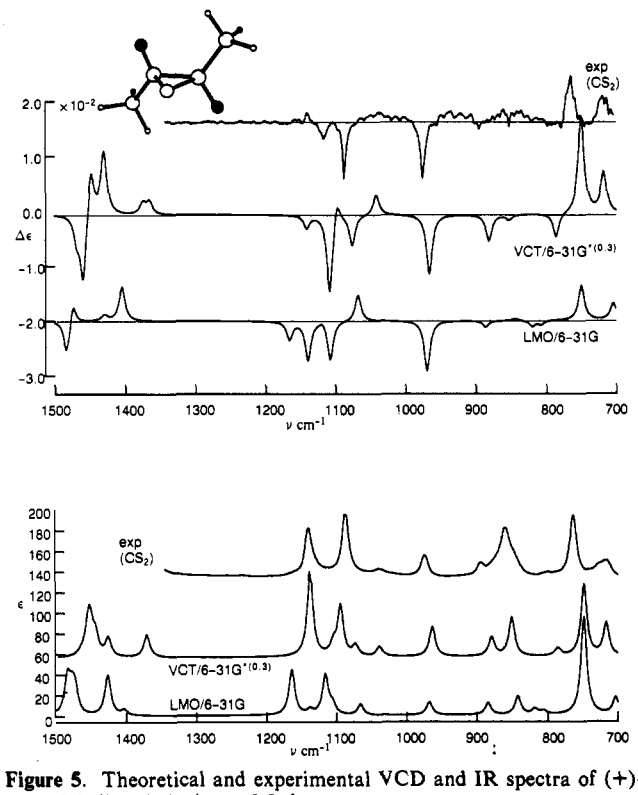

Figure 5. Theoretical and experimental VCD and IR spectra of (+)-*trans*-2,3-dimethyloxirane-2,3-d_2.

Acknowledgment. Grants from the NIH (GM29375), NSF (CHE8808018), and NSERCC are gratefully acknowledged.

(37) Foster, J. M.; Boys, S. F. *Rev. Mod. Phys.* **1960**, *32*, 300–302.
(38) (a) Schmidt, M. W.; Boatz, J. A.; Baldridge, K. K.; Koseki, S.; Gordon, M. S.; Eldbert, S. T.; Lam, B. *QCPE Bull.* **1987**, *7*, 115. (b) Dupuis, M.; Spangler, D.; Wendoloski, J. J. *NRCC Program QGO1*; University of California: Berkeley, CA, 1980.
(39) Polavarapu, P. L. *Chem. Phys. Lett.* **1990**, *171*, 271–276.
(40) Pople, J. A.; Schlegel, H. B.; Krishnan, R.; De Frees, D. J.; Binkley, J. S.; Frisch, M. J.; Whiteside, R. A.; Hout, R. F.; Hehre, W. J. *Int. J. Quantum Chem., Quantum Chem. Symp.* **1981**, *15*, 269.